AN INDEPENDENT ACTIVE TORQUE BALANCER USING A SERVO-CONTROLLED DIFFERENTIAL GEAR TRAIN

Sun Jing and Yao Yan-An
School of Mechanical and Electronic Control Engineering, Beijing Jiaotong University, Beijing 100044, P.R. CHINA
E-mail: yayao@bjtu.edu.cn

Received January 2009, Accepted April 2009
No. 09-CSME-01, E.I.C. Accession 3087

ABSTRACT

This paper proposes a novel concept of active balancer for reducing the input torque fluctuations of mechanisms. A differential gear train is used in this active balancer and one of its two input shafts is driven and controlled by a servomotor. From the structural point of view, it is designed as an independent device that can be assembled and disassembled easily; from the functional point of view, it can minimize the torque fluctuations in a variety of working conditions. At first, an exact control function of the servomotor that can totally eliminate the input torque fluctuations of the mechanism is gained by an analytical method; in what follows, an optimization approach is developed to select appropriate control functions for the servomotor to balance the input torque of the working mechanism with consideration of the servomotor's own input torque minimization; finally, an integrated method is presented for optimizing both the control function of the servomotor and the structure parameters of the differential gear train. Two numerical examples are given to illustrate the design procedure and to show its feasibility.

EQUILIBREUR/STABILISATEUR ACTIF DE COUPLE INDEPENDANT UTILISANT UN SERVOMOTEUR CONTROLE PAR UN TRAIN D'ENGRENAGES DIFFERENTIEL

RÉSUMÉ

Cette contribution propose un nouveau concept d'équilibreur/de stabilisateur actif pour la réduction des fluctuations du couple d'entrée des mécanismes. Cet équilibreur/stabilisateur actif est constitué d'un train d'engrenages différentiel et un de ses deux arbres d'entrée est actionné et contrôlé par un servomoteur. D'un point de vue structurel, l'équilibreur/le stabilisateur est conçu comme un dispositif indépendant qui peut être monté et démonté facilement ; d'un point de vue fonctionnel, il est capable de minimiser les fluctuations de couple pour des conditions de fonctionnement variés. Dans un premier temps, une fonction exacte de contrôle du servomoteur, capable d'éliminer totalement la fluctuation du couple d'entrée du mécanisme, est obtenue par une méthode d'analyse; ensuite, une approche d'optimisation est mise au point afin de sélectionner les fonctions de contrôle du servomoteur pour l'équilibrage du couple d'entrée du mécanisme en fonctionnement tout en considérant la minimisation du couple d'entrée propre au servomoteur; enfin, une méthode intégrée est présentée pour optimiser à la fois la fonction de contrôle du servomoteur et les paramètres de structure du train d'engrenages différentiel. Deux exemples numériques sont donnés pour illustrer la procédure de conception et démontrer sa faisabilité.

1. INTRODUCTION

A basic assumption during mechanism design is that the mechanism is operated with a constant driving speed. However, there is an unwanted speed fluctuation in mechanism as a result of the variation of input torque. This phenomena increases vibration and noise levels, shortens fatigue life, induces wear and makes the mechanism work in poor accuracy. Input torque balancing is an effective measure in coping with this problem.

Internal mass redistribution discussed by Berkof [1] is a simple and classical way for input torque balancing. It is classified as ‘‘passive balancing’’ method by Kochev [2] for the reason of optimizing inertial parameters of the mechanism. According to Kochev’s classification, the ‘‘active balancing’’ methods are adding links, gears, dyads or more complex devices to the working mechanisms. There are many literatures on this type of methods. Liu and Huang [3] adopt two-link dyad to balance the fluctuation of the input torque. Nishioka [4,5] proposes several cam or spring based mechanisms to compensate the torque variations of cam mechanisms. Funk and Han [6] describe a device that consists of a gear pair, a closed-track cam and a rotating member. Dooner [7] uses a noncircular gear pair to create an auxiliary torque fluctuation for reducing the torque fluctuation. Noncircular gears are also being investigated for the aim of input torque balancing by Yao and Yan [8]. Demeulenaere et al. [9–11] achieve torque balancing by using a cam-based centrifugal pendulum. Analogously, different devices are developed for torque balancing in Refs. [12–15].

With the approaches above, the input torque fluctuations of mechanisms surely can be reduced partially or even completely. However, most of the auxiliary devices are designed for different mechanisms. The balancing effect of each device which designed for one mechanism may become worse when it is used in other mechanisms. Besides, owing to the inescapable errors of manufacturing and assembling, the mechanisms in practice may not coincide with the designed one, so do the adding devices. Therefore, the results of balancing the input torque may be far away from the theory. Furthermore, if the working condition of the mechanism is changed, the balancing device may not be adapted accordingly and another device should be designed.

Currently, several more active methods are studied. These methods introduce the control system to the machine. Yao et al. [16] employ a servomotor to drive the input link of a linkage mechanism for balancing the input torque. Thuemmel et al. [17,18] analyze a balancing method by actively controlling redundant drivers. Zhang et al. [19] obtain torque balancing by adding a servomotor-controlled five-bar linkage to the working mechanism.

In this paper, an active balancer which consists of a differential gear train and a servomotor is presented. This balancer has the advantages of both the gears and the active methods. With the compact structure and the good dynamic performance as gears, the active balancer can be fixed on any suitable shaft of the machine, conveniently to be used and easily to be installed and uninstalled. With the control of the servomotor, the active balancer can meet the changed working condition and the altered mechanism.

2. ACTIVE BALANCER

Fig.1a shows a working platform with the proposed active balancer. An original motor **7**, a speed reducer **8**, a working mechanism which needs to be balanced and an active balancer are included in this system. Here, a crank-rocker mechanism is taken as the example of the working mechanism, and it contains the crank **1**, the link **2** and the rocker **3**. The active balancer consists

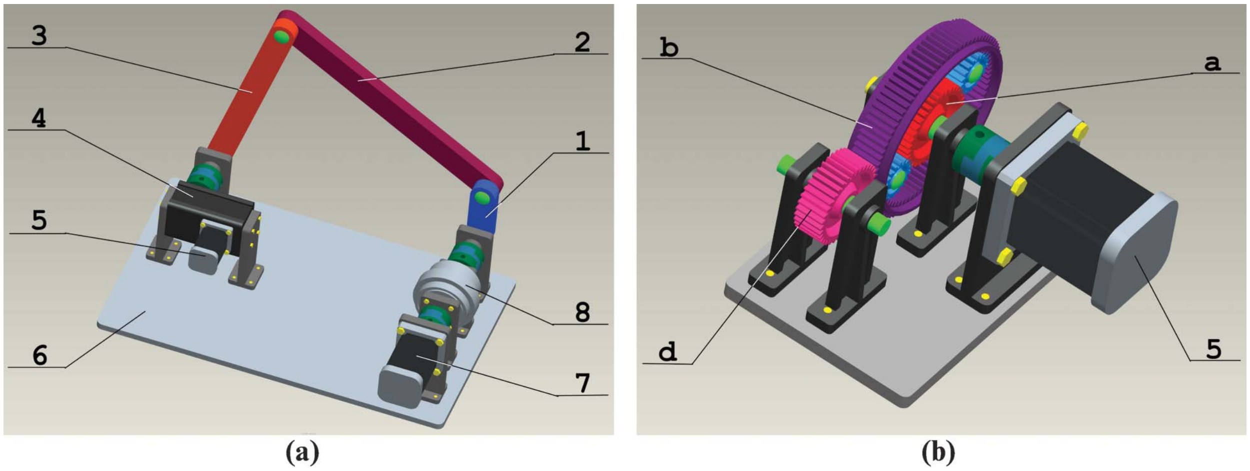

Fig. 1. The three-dimensional model of the active balancer (a) A working platform with the active balancer, (b) The internal structure of the active balancer **1**-the crank, **2**-the link, **3**-the rocker, **4**-the two-DOF mechanism, **5**-the servomotor, **6**-the working platform, **7**-the original motor, **8**-the speed reducer, **a**-the sun gear, **b**-the internal ring gear, **d**-the fixed axis gear

of a two-degree of freedom (DOF) mechanism **4** and a servomotor **5**. In this paper, the active balancer is installed on the output shaft of the crank-rocker mechanism.

The input shaft of the crank-rocker mechanism in this system is driven by the original motor **7** through the speed reducer **8**. The output shaft of the crank-rocker mechanism is connected with one of the two input shafts of the two-DOF mechanism **4**. The other input shaft of the two-DOF mechanism **4** is driven by the servomotor **5**. Through designing a suitable control function for the servomotor, the input torque of the crank-rocker mechanism can be balanced by this active balancer. Since one of the two input shafts of the two-DOF mechanism is driven by the output member of the crank-rocker mechanism, the active balancer will not interfere with the kinematics characteristics of the crank-rocker mechanism, but just improve the dynamics characteristics of the crank-rocker mechanism. Additionally, this active balancer can be assembled and disassembled conveniently.

The internal structure of the active balancer is shown in Fig.1b. A differential gear train is used here as the two-DOF mechanism. The servomotor **5** drives one of the two input shafts of the differential gear train and this shaft is fixed to the center of the sun gear **a**. From Fig.1b, you also can see the internal ring gear **b** of the differential gear train has teeth on both sides, and those outer ones mesh the teeth of a fixed axis gear **d**. The fixed axis gear **d** is installed on the output shaft of the crank-rocker mechanism. This active balancer can be used for different mechanisms whose input torque needs to be balanced. So here the crank-rocker mechanism can be taken place by any other mechanism.

The scheme of a crank-rocker mechanism with the active balancer is displayed in Fig.2. The crank **1** which is the input member of the crank-rocker mechanism is driven by the original motor through the shaft $\mathbf{O_1}$. The rocker **3** and the fixed axis gear **d** are both connected with the shaft $\mathbf{O_3}$, and this shaft is not only the output shaft of the crank-rocker mechanism, but also the one of the two input shafts of the differential gear train. The other input shaft of differential gear train $\mathbf{O_a}$, which is joined with the center of the sun gear **a**, is driven by the servomotor. A reference coordinate is chosen with $\mathbf{O_1}$ as the origin. Symbols φ_1 and φ_a represent the angular displacements of the two input parts respectively. φ_2 and φ_3 represent the angular displacements

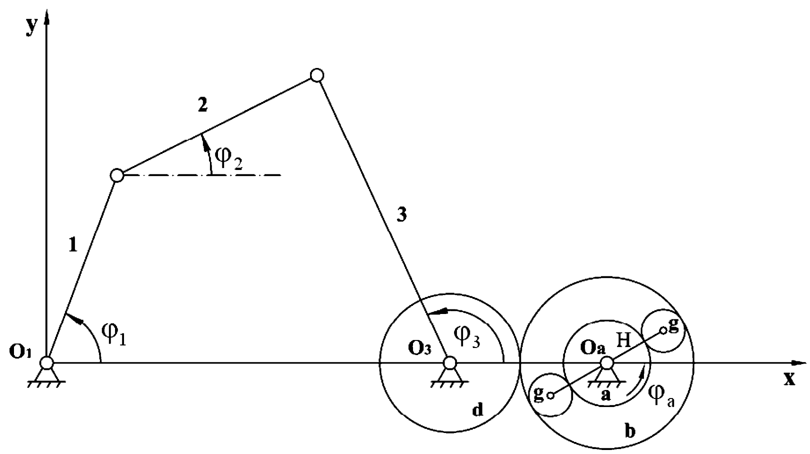

Fig. 2. The scheme of a system with the active balancer **1**-the crank, **2**-the link, **3**-the rocker, **d**-the fixed axis gear **a**-the sun gear, **b**-the internal ring gear, **g**-the planetary gear, **H**-the planetary carrier

of the link **2** and the rocker **3** respectively. This section will derive an exact control function of the servomotor for eliminating the input torque fluctuation completely through an analytical way.

Some assumptions are made for simplifying the mathematical model:

1) Friction and gravity forces are negligible;
2) Joint clearances are negligible;
3) Each moving part of the system is rigid and homogeneous;
4) The centers of mass for all parts are on their own geometric centers;
5) Crank **1** which is driven by the original motor rotates at a constant angular velocity.

2.1 The input torque of the system without active balancer

There is only a crank-rocker mechanism in the system without the active balancer.

The kinetic energy of the crank-rocker mechanism E_1 is expressed as

$$E_1 = \frac{1}{2}\left(J_1'\dot{\varphi}_1^2 + J_2\dot{\varphi}_2^2 + m_2\dot{x}_2^2 + m_2\dot{y}_2^2 + J_3'\dot{\varphi}_3^2\right), \tag{1}$$

where J_1' and J_3' are the moments of inertia of the crank **1** and the rocker **3** with respect to $\mathbf{O_1}$ and $\mathbf{O_3}$ respectively. J_2 is the moment of inertia of the link **2** with respect to the centroid of it. $\dot{\varphi}_1$, $\dot{\varphi}_2$ and $\dot{\varphi}_3$ are angular velocities of parts **1**, **2** and **3**, so $\dot{\varphi}_1 = d\varphi_1/dt$, $\dot{\varphi}_2 = d\varphi_2/dt$ and $\dot{\varphi}_3 = d\varphi_3/dt$. m_2 is the mass of the link **2**. $\dot{x}_2$ and $\dot{y}_2$ are x- and y-components of velocity for the centroid of link **2**. Here, $\dot{\varphi}_2$ and $\dot{\varphi}_3$ can be expressed as functions of $\dot{\varphi}_1$:

$$\dot{\varphi}_2 = g_2(\varphi_1)\cdot\dot{\varphi}_1, \tag{2a}$$

$$\dot{\varphi}_3 = g_3(\varphi_1)\cdot\dot{\varphi}_1, \tag{2b}$$

where

$$g_2(\varphi_1) = \frac{l_1\cdot\sin(\varphi_1 - \varphi_3)}{l_2\cdot\sin(\varphi_3 - \varphi_2)}, \tag{3a}$$

$$g_3(\varphi_1)=\frac{l_1\cdot\sin(\varphi_1-\varphi_2)}{l_3\cdot\sin(\varphi_3-\varphi_2)}. \tag{3b}$$

$\dot{x}_2$ and $\dot{y}_2$ can be expressed as functions of $\dot{\varphi}_1$ too. Let J_e be the equivalent moment of inertia of this system, the kinetic energy E_1 can be written as

$$E_1=\tfrac{1}{2}J_e(\varphi_1)\dot{\varphi}_1^2. \tag{4}$$

So the input torque of this system $M_1{}'$ can be formulated as follows:

$$M_1{}'=\frac{dE_1}{d\varphi_1}=\frac{d}{d\varphi_1}\left(\frac{1}{2}J_e(\varphi_1)\dot{\varphi}_1^2\right)=\frac{1}{2}\frac{d(J_e(\varphi_1))}{d\varphi_1}\dot{\varphi}_1^2. \tag{5}$$

2.2. The input torque of the system with active balancer

The system with the active balancer as shown in Fig. 2 includes a differential gear train and a crank-rocker mechanism. Since the motion of this two-DOF system can be determined by φ_1 and φ_a, we chose φ_1 and φ_a as the generalized coordinates of this system. Then we have $q_1=\varphi_1$ and $q_2=\varphi_a$. Correspondingly, the generalized velocities are $\dot{q}_1=\dot{\varphi}_1$ and $\dot{q}_2=\dot{\varphi}_a$ and the generalized accelerations are $\ddot{q}_1=\ddot{\varphi}_1$ and $\ddot{q}_2=\ddot{\varphi}_a$.

The Lagrange's equation for this system should be written as

$$\frac{d}{dt}\left(\frac{\partial E}{\partial \dot{q}_j}\right)-\frac{\partial E}{\partial q_j}=F_j, \quad (j=1,2) \tag{6}$$

in which, F_j are the generalized forces. E is the kinetic energy of the whole system, which is the sum of the kinetic energy of all moving parts. It can be written as

$$E=E_1+E_2. \tag{7}$$

E_2 is the kinetic energy of the differential gear train. Here, it can be expressed as

$$E_2=\tfrac{1}{2}\left(\sum J_i\dot{\varphi}_i^2+nJ_g\dot{\varphi}_g^2+nJ_{gg}\dot{\varphi}_H^2\right). \quad i=a,H,b,d \tag{8}$$

In this expression, J_a, J_H, J_b, J_d and J_g are the moments of inertia with respect to the centers of mass for parts **a**, **H**, **b**, **d** and **g** respectively. $\dot{\varphi}_a$, $\dot{\varphi}_H$, $\dot{\varphi}_b$, $\dot{\varphi}_d$ and $\dot{\varphi}_g$ are angular velocities of parts **a**, **H**, **b**, **d** and **g** respectively. n is the number of the planetary gears. It is worth noting that the planetary gear of the differential gear train revolves around not only the center of itself but also the center of the sun gear. Hence, the planetary gear has moments of inertia with respect to both its own centroid and the centroid of the sun gear. The moment of inertia with respect to the centroid of the sun gear is denoted by J_{gg}. The angular velocity of this revolution equals the angular velocity of planetary carrier $\dot{\varphi}_H$.

Since the fixed axis gear **d** is fixed with the rocker **3**, we get $\varphi_d=\varphi_3$. Here, $\dot{\varphi}_g$, $\dot{\varphi}_H$, $\dot{\varphi}_b$ and $\dot{\varphi}_d$ can be expressed as functions of $\dot{\varphi}_a$ and $\dot{\varphi}_3$:

$$\dot{\varphi}_g=k_1\dot{\varphi}_a+k_2\dot{\varphi}_3, \tag{9a}$$

$$\dot{\varphi}_H = k_3\dot{\varphi}_a + k_4\dot{\varphi}_3, \tag{9b}$$

$$\dot{\varphi}_b = k_5\dot{\varphi}_3, \tag{9c}$$

$$\dot{\varphi}_d = \dot{\varphi}_3, \tag{9d}$$

where

$$k_1 = -[za/(zb - za)], \tag{10a}$$

$$k_2 = -[zb \cdot zd/(zb - za) \cdot zc], \tag{10b}$$

$$k_3 = za/(za + zb), \tag{10c}$$

$$k_4 = -[zb \cdot zd/(za + zb) \cdot zc], \tag{10d}$$

$$k_5 = -zd/zc. \tag{10e}$$

Here, za and zd are the teeth numbers of the sun gear **a** and the fixed axis gear **d** respectively. zb and zc are the teeth numbers of the internal ring gear's inside teeth and outside teeth respectively.

Then, the motion of differential gear train can be determined by $\dot{\varphi}_3$ and $\dot{\varphi}_a$. Let J_{11}', J_{12}' and J_{22}' be the equivalent moments of inertia of the differential gear train, E_2can be written as

$$E_2 = \frac{1}{2}J_{11}'\dot{\varphi}_3^2 + J_{12}'\dot{\varphi}_3\dot{\varphi}_a + \frac{1}{2}J_{22}'\dot{\varphi}_a^2, \tag{11}$$

in which,

$$J_{11}' = J_d + J_b k_5^2 + nJ_g k_2^2 + nJ_{gg} k_4^2 + J_H k_4^2, \tag{12a}$$

$$J_{12}' = nJ_g k_1 k_2 + nJ_{gg} k_3 k_4 + J_H k_3 k_4, \tag{12b}$$

$$J_{22}' = J_a + nJ_g k_1^2 + nJ_{gg} k_3^2 + J_H k_3^2. \tag{12c}$$

Substituting $\dot{q}_1 = \dot{\varphi}_1$, $\dot{q}_2 = \dot{\varphi}_a$, equation (2b) ,equation (4) and equation (11) into equation (7), we obtain the total kinetic energy E which can be written in terms of q_1, q_2, $\dot{q}_1$ and $\dot{q}_2$:

$$E = \frac{1}{2}J_{11}\dot{q}_1^2 + J_{12}\dot{q}_1\dot{q}_2 + \frac{1}{2}J_{22}\dot{q}_2^2, \tag{13}$$

where J_{11}, J_{12} and J_{22} denotes the equivalent moments of inertia of the system with active balancer. They can be derived as follows:

$$J_{11} = J_{11}' \cdot g_3^2(\varphi_1) + J_e(\varphi_1), \tag{14a}$$

$$J_{12} = J_{12}' \cdot g_3(\varphi_1), \tag{14b}$$

$$J_{22} = J_{22}'. \tag{14c}$$

Taking the partial derivatives with respect to q_1, q_2, $\dot{q}_1$ and $\dot{q}_2$ of the equation (13) respectively, we can obtain $\frac{\partial E}{\partial q_j}$ and $\frac{\partial E}{\partial \dot{q}_j}$ $(j = 1,2)$. Calculating the partial derivatives of $\frac{\partial E}{\partial \dot{q}_j}$ with respect to$t$, and substituting the results into equation (6), the differential equation of motion for this system can be derived as

$$\left.\begin{aligned} J_{11}\ddot{q}_1 + J_{12}\ddot{q}_2 + \frac{1}{2}\frac{\partial J_{11}}{\partial q_1}\dot{q}_1^2 + \frac{\partial J_{11}}{\partial q_2}\dot{q}_1\dot{q}_2 + \left(\frac{\partial J_{12}}{\partial q_2} - \frac{1}{2}\frac{\partial J_{22}}{\partial q_1}\right)\dot{q}_2^2 = F_1 \\ J_{22}\ddot{q}_2 + J_{12}\ddot{q}_1 + \left(\frac{\partial J_{12}}{\partial q_1} - \frac{1}{2}\frac{\partial J_{11}}{\partial q_2}\right)\dot{q}_1^2 + \frac{\partial J_{22}}{\partial q_1}\dot{q}_1\dot{q}_2 + \frac{1}{2}\frac{\partial J_{22}}{\partial q_2}\dot{q}_2^2 = F_2 \end{aligned}\right\}. \tag{15}$$

Since friction, gravity and other external forces of this system are assumed to be disregarded; all the external forces and torques applied here are the input torques of the original motor M_1 and the servomotor M_a. They drive the crank **1** and the sun gear **a** respectively. According to the Generalized Principle of Virtual Work, the power of this system can be written as

$$P = F_1\dot{q}_1 + F_2\dot{q}_2 = M_1\dot{q}_1 + M_a\dot{q}_2 = M_1\dot{\varphi}_1 + M_a\dot{\varphi}_a, \tag{16}$$

where the two input torques M_1 and M_a equal F_1 and F_2 respectively.

So, M_1 and M_a can be derived as

$$M_1 = J_{11}\ddot{q}_1 + J_{12}\ddot{q}_2 + \frac{1}{2}\frac{\partial J_{11}}{\partial q_1}\dot{q}_1^2 + \frac{\partial J_{11}}{\partial q_2}\dot{q}_1\dot{q}_2 + \left(\frac{\partial J_{12}}{\partial q_2} - \frac{1}{2}\frac{\partial J_{22}}{\partial q_1}\right)\dot{q}_2^2, \tag{17a}$$

$$M_a = J_{22}\ddot{q}_2 + J_{12}\ddot{q}_1 + \left(\frac{\partial J_{12}}{\partial q_1} - \frac{1}{2}\frac{\partial J_{11}}{\partial q_2}\right)\dot{q}_1^2 + \frac{\partial J_{22}}{\partial q_1}\dot{q}_1\dot{q}_2 + \frac{1}{2}\frac{\partial J_{22}}{\partial q_2}\dot{q}_2^2. \tag{17b}$$

According to equation (14), the partial derivatives of J_{11}, J_{12} and J_{22} with respect to q_1 and q_2 can be derived as

$$\frac{\partial J_{11}}{\partial q_1} = 2 \cdot g_3(\varphi_1) \cdot J_{11}' \cdot \frac{d(g_3(\varphi_1))}{d\varphi_1} + \frac{d(J_e(\varphi_1))}{d\varphi_1}, \tag{18a}$$

$$\frac{\partial J_{12}}{\partial q_1} = J_{12}' \cdot \frac{d(g_3(\varphi_1))}{d\varphi_1}, \tag{18b}$$

$$\frac{\partial J_{11}}{\partial q_2} = \frac{\partial J_{12}}{\partial q_2} = \frac{\partial J_{22}}{\partial q_1} = \frac{\partial J_{22}}{\partial q_2} = 0. \tag{18c}$$

Then, we obtain the expressions of M_1 and M_a as follows:

$$M_1 = J_{11}\ddot{\varphi}_1 + J_{12}\ddot{\varphi}_a + J_{11}'\cdot g_3(\varphi_1)\cdot\frac{d(g_3(\varphi_1))}{d\varphi_1}\cdot\dot{\varphi}_1^2 + M_1', \tag{19a}$$

$$M_a = J_{22}\ddot{\varphi}_a + J_{12}\ddot{\varphi}_1 + J_{12}'\cdot\frac{d(g_3(\varphi_1))}{d\varphi_1}\cdot\dot{\varphi}_1^2. \tag{19b}$$

Besides, there is a assumption that the crank **1** rotates at a constant angular velocity, so in this system, $\ddot{\varphi}_1 = \ddot{q}_1 = 0$. Then, it follows that:

$$M_1 = J_{12}'\cdot g_3(\varphi_1)\cdot\ddot{\varphi}_a + J_{11}'\cdot g_3(\varphi_1)\cdot\frac{d(g_3(\varphi_1))}{d\varphi_1}\cdot\dot{\varphi}_1^2 + M_1', \tag{20a}$$

$$M_a = J_{22}'\ddot{\varphi}_a + J_{12}'\cdot\frac{d(g_3(\varphi_1))}{d\varphi_1}\cdot\dot{\varphi}_1^2. \tag{20b}$$

According to equation (20a), when

$$g_3(\varphi_1) \neq 0, \tag{21}$$

if

$$\ddot{\varphi}_a = \ddot{q}_1 = -(J_{11}'\cdot g_3(\varphi_1)\cdot\frac{d(g_3(\varphi_1))}{d\varphi_1}\cdot\dot{\varphi}_1^2 + M_1')/J_{12}'\cdot g_3(\varphi_1), \tag{22}$$

the input torque of the original motor in the system with active balancer will equal zero:

$$M_1 = 0. \tag{23}$$

When

$$g_3(\varphi_1) = 0, \tag{24}$$

we have

$$M_1 = M_1'. \tag{25}$$

According to the equation (3b), if

$$\varphi_1 - \varphi_2 = n\pi \quad (n \in Z), \tag{26}$$

the equation (24) can be satisfied. This conclusion indicates that if the crank-rocker mechanism is on the extreme positions, the input torque M_1 just equal M_1' and will not be changed by the active balancer.

From the above analysis, when the crank-rocker mechanism is not on the extreme positions, a control function of the servomotor just like equation (22) that can completely eliminate the fluctuations of M_1 is obtained. When the crank-rocker mechanism is on the extreme positions, the input torque M_1 will equal M_1'. That means in the complete balancing situation, the curve of the input torque M_1 will have sudden changed points. In order to make the curve of the input torque M_1 smoothly and reduce the fluctuations of M_a simultaneously, two optimization approaches are developed in the next section.

3. OPTIMIZATION PROCESS

In order to smooth the curve of the input torque M_1 and avoid burdening the servo control system excessively, two optimization approaches are proposed in this section to meet the requirements of reducing the fluctuations of both M_1 and M_a. The first method is to select suitable control functions with acceptable variations for the servomotor. The second method is integrated design of both the control function of the servomotor and the structure parameters of the differential gear train.

3.1. Control function design

An optimization procedure is designed as follows for finding a suitable control function of the servomotor.

3.1.1. Objective function

The objective function is defined as

$$F(x) = \omega_1 f_1(x) + \omega_2 f_2(x), \tag{27a}$$

where

$$f_1(x) = \frac{1}{2\pi}\int_0^\tau |M_a|^2 \dot{\varphi}_1^2 dt, \tag{27b}$$

$$f_2(x) = \frac{1}{2\pi}\int_0^\tau |M_1|^2 \dot{\varphi}_1^2 dt \Big/ \frac{1}{2\pi}\int_0^\tau |M_1'|^2 \dot{\varphi}_1^2 dt \tag{27c}$$

are used to minimize the root-mean-square (RMS) values of the input torque M_a and M_1. τ is the period for a complete motion cycle. ω_1 and ω_2 are weighting factors which can be adjusted to meet the various design requirements. A trial-and-error procedure is needed to find the appropriate weighting factors here. The aim of this optimization design is to minimize the value of $F(x)$.

3.1.2. Design constraints

In what follows, design constraints are developed for this procedure.

The sun gear **a** which is driven by the servomotor should rotate one revolution in a period τ. Therefore, we have

$$\varphi_a(\tau) - \varphi_a(0) = 2\pi. \tag{28a}$$

Considering the continuity of the input motion, the angular displacement function should be at least second-order differentiable. This continuity condition can be formulated by

$$\dot{\varphi}_a(\tau) = \dot{\varphi}_a(0), \tag{28b}$$

$$\ddot{\varphi}_a(\tau) = \ddot{\varphi}_a(0). \tag{28c}$$

3.1.3. Design variables

The speed trajectory $\dot{\varphi}_a$ can be expressed as a polynomial function like

$$\dot{\varphi}_a(t) = \sum_{i=1}^{10} C_i t^{i-1}, \quad t \in [0,\tau] \tag{29a}$$

Taking the integral and derivation with respect to time$t$respectively leads to

$$\varphi_a(t) = C_0 + \sum_{i=1}^{10} \frac{1}{i} C_i t^i, \quad t \in [0,\tau] \tag{29b}$$

$$\ddot{\varphi}_a(t) = \sum_{i=2}^{10} (i-1) C_i t^{i-2}, \quad t \in [0,\tau] \tag{29c}$$

where the coefficients C_0, C_1, C_2, ..., C_{10} are determined by the optimization approach for selecting a suitable control function for the servomotor. According to equation (28a), C_0 can be eliminated.

So the design variables can be expressed as

$$X = [C_1, C_2, \ldots, C_{10}]. \tag{30}$$

Since the equality constraints can be eliminated by an algebraic method, this optimization problem can be solved by using the fminsearch function of the Matlab Optimization Toolbox. This function applies Simplex algorithm and gets struck in local optima.

3.2. Integrated design of structural parameters and control function

By optimizing the control function of the servomotor, we can certainly gain feasible results for the system whose input torque needs to be balanced. However, if the structure parameters of the differential gear train are optimized simultaneously, we can obtain better results for the same system rather than feasible results.

The method of integrated design studies how to design the control function and the structural parameters simultaneously. The goal of this optimization procedure is to find a result that includes a set of suitable structural parameters of the differential gear train and an appropriate control function of the servomotor for the whole system.

The objective function of this method is just the same as equation (27).

3.2.1. Design constraints

The design constraints for the control function are the same as equation (28).

The analysis of the design constraints for the structure parameters is listed as follows.

First of all, J_ε ($\varepsilon = a, g, gg, H, b, d$) should be positive, so we have constraints:

$$J_\varepsilon > \delta. \quad (\delta > 0) \tag{31}$$

Since the moments of inertia can neither equal zero nor less than zero, δ is a random positive value that should be decided according to the situations of practice.

Furthermore, in order to keep the gears not to be undercut, the teeth numbers of them should be no less than 17. So, at first, we have:

$$za > 17, \tag{32}$$

$$zd > 17. \tag{33}$$

According to the relationship of za, zb and the planetary gear's teeth number zg, it follows that:

$$zg = \frac{1}{2}(zb - za) > 17. \tag{34}$$

Then, another constraint is gained:

$$zb - za > 34. \tag{35}$$

The constraint of the relationship between zb and zc is analyzed as follows.

As shown in Fig.3, R_{ba}, R_b and R_{bf} are the representations of the addendum circle radius, the pitch circle radius and the dedendum circle radius of the inside teeth of the internal ring gear respectively. Moreover, R_{ca}, R_c and R_{cf} are the representations of the addendum circle radius, the pitch circle radius and the dedendum circle radius of the outside teeth respectively. Then, a relationship should be satisfied:

$$R_{cf} > R_{bf}. \tag{36}$$

In which,

$$R_{bf} = R_b + M({h_a}^* + c^*) = \frac{1}{2} M \cdot zb + M({h_a}^* + c^*), \tag{37a}$$

$$R_{cf} = R_c - M({h_a}^* + c^*) = \frac{1}{2} M \cdot zc - M({h_a}^* + c^*), \tag{37b}$$

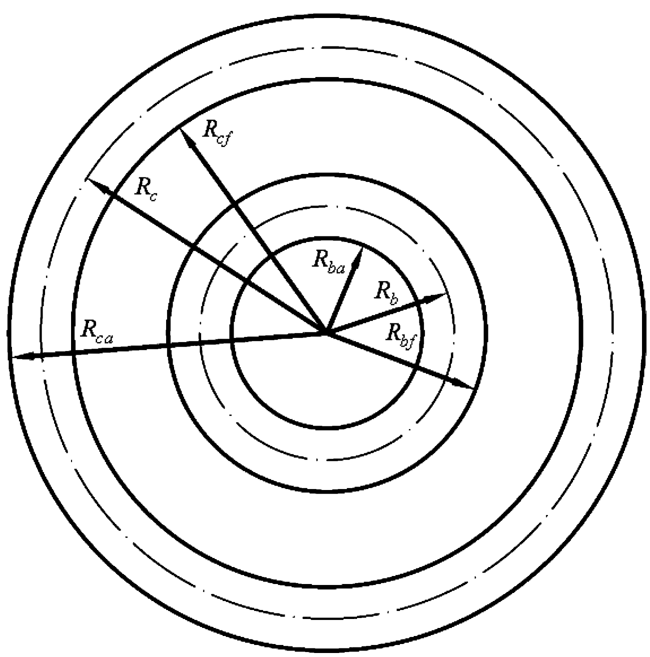

Fig. 3. The scheme of the relationship between zb and zc

where $h_a{}^*$ is the addendum coefficient, c^* is the tip clearance coefficient and M is the modulus of the gears. Let $h_a{}^*=1$ and $c^*=0.25$. Substituting equation (37) into equation (36), another constraint is obtained:

$$zc - zb > 5 + k, \quad (k > 0 \text{ and } k \in Z) \tag{38}$$

where k is a random positive integer that should be decided according to the situations of practice.

3.2.2. Design variables

According to equation (30) and the analysis in section 3.2.1, the design variables of the integrated design can be written as:

$$X = \left[C_1, C_2, ..., C_{10}, J_g, J_{gg}, J_H, J_d, J_b, J_a, za, zb, zc, zd\right]. \tag{39}$$

This optimization problem is a nonlinear constraint optimization problem, so the fmincon function of the Matlab Optimization Toolbox can be used to solve it. This function includes a Sequential Quadratic Programming (SQP) technique and also gets a local optimal solution.

4. DESIGN EXAMPLES

In this section, two examples are given to demonstrate the design procedure. Example 1 displays the optimization design of the control function of the servomotor. Example 2 describes the integrated design of both the structure parameters of the differential gear train and the control function of the servomotor.

4.1. Example 1

With the data listed in Table 1, two different crank-rocker mechanisms are formed as the working mechanisms of this example. In example 1.1, optimization results of the control functions are gained by balancing the first crank-rocker mechanism. Example 1.2 shows the effects that using the control functions optimized for the first crank-rocker mechanism to balance the second crank-rocker mechanism. Example 1.3 displays the process of redesigning the control functions for the second crank-rocker mechanism.

The angular velocity of the crank **1** which is driven by the original motor is 30*rpm* constantly.

The structure parameters of the differential gear train used in this example are shown in Table 2. Moreover, the number of planetary gears equals 2.

Table 1 Parameters of the crank-rocker mechanism

		Crank **1**	Link **2**	Rocker **3**	Link **4**
1	Length (m)	0.12	0.4	0.28	0.45
	Mass (kg)	0.1	0.8	0.4	
2	Length (m)	0.08	0.4	0.3	0.52
	Mass (kg)	0.08	0.8	0.5	

4.1.1. Example 1.1

The results of this optimization procedure are shown in Fig.4, Tables 3 and 5. These data is obtained by using the parameters of the first crank-rocker mechanism in Table 1 and the structure parameters of the differential gear train in Table 2. Due to equation (28), three of the design variables which listed in equation (30) can be eliminated. Here, we eliminate C_8, C_9 and C_{10}. There are two cases in this example: $\omega_1 = 0$, $\omega_2 = 1$ and $\omega_1 = 0.01$, $\omega_2 = 0.99$.

In the case $\omega_1 = 0$, $\omega_2 = 1$, if we only minimize the fluctuation of M_1 with the optimization procedure, we can get improved results as showed in Fig.4 and Table 3. The improvements are 90.96%, 15.49% and 81.86% for the RMS value, the maximal value and the minimal value of M_1 respectively. Nevertheless, as shown in Fig.4b, the fluctuation of M_a in this case is too large. In the case $\omega_1 = 0.01$, $\omega_2 = 0.99$, the optimization design for the fluctuations of both M_1 and M_a is carried out. The improvements of M_1 are 42.71%, 6.66% and 43.65% for the RMS value, the maximal value and the minimal value respectively. The improvements of 92.10%, 60.16% and 70.74% for the RMS value, the maximal value and the minimal value of M_a respectively are also gained by reducing the improvements of M_1. These reductions are 53.05%, 57% and 46.68% for the RMS value, the maximal value and the minimal value of M_1 respectively. These analytical

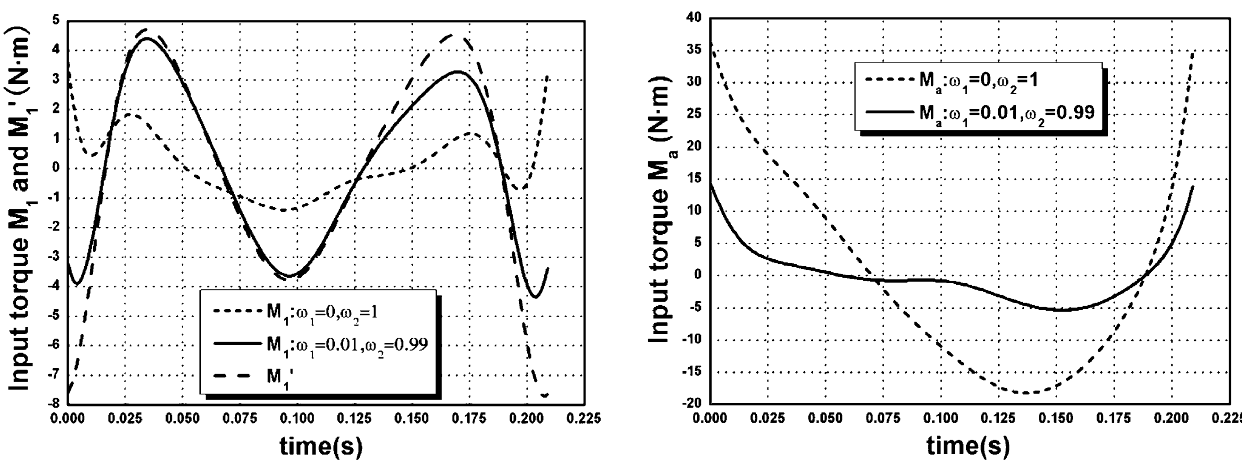

(a) Input torque M_1 and M_1' **(b) Input torque M_a**

Fig. 4. Design results of example 1.1

Table 2 Parameters of the differential gear train

	Teeth number	Moment of Inertia (kg·m^2)
Sun gear **a**	36	$J_a = 1.088 \times 10^{-4}$
Planetary gear **g**	18	$J_g = 7.622 \times 10^{-6}$
		$J_{gg} = 5.706 \times 10^{-5}$
Internal gear **b**	Inside: 72 Outside: 84	$J_b = 2.02 \times 10^{-3}$
Fixed axis gear **d**	36	$J_d = 1.068 \times 10^{-4}$
Planetary carrier **H**		$J_H = 2.199 \times 10^{-1}$

Table 3 Data of the results for example 1

	Example 1.1		Example 1.2		Example 1.3	
	$\omega_1 = 0$ $\omega_2 = 1$	$\omega_1 = 0.01$ $\omega_2 = 0.99$	$\omega_1 = 0$ $\omega_2 = 1$	$\omega_1 = 0.01$ $\omega_2 = 0.99$	$\omega_1 = 0$ $\omega_2 = 1$	$\omega_1 = 0.01$ $\omega_2 = 0.99$
$F(x)$	0.0904	0.7628	3.9587	0.9233	0.1387	0.6615
$f_1(x)$	247.7732	19.5635	341.6020	50.5996	134.8528	22.9501
$f_2(x)$	0.0904	0.5729	0.5481	0.4215	0.1387	0.4364
$M_1{}'_{max}$ (N·m)	4.7105	4.7105	2.1813	2.1813	2.1813	2.1813
$M_1{}'_{min}$ (N·m)	−7.7005	−7.7005	−2.4542	−2.4542	−2.4542	−2.4542
M_{1max} (N·m)	3.9808	4.3970	4.1853	1.8193	1.5707	1.6217
M_{1min} (N·m)	−1.3970	−4.3396	−1.5796	−1.6842	−0.8622	−1.5921
M_{amax} (N·m)	38.3290	15.2715	43.6682	20.6106	26.4036	10.4888
M_{amin} (N·m)	−18.2153	−5.3289	−19.8669	−7.7195	−13.9637	−6.7405

Table 4 Data of the results for example 2

	$\omega_1 = 0$, $\omega_2 = 1$		$\omega_1 = 0.01$, $\omega_2 = 0.99$	
	Before rounding	After rounding	Before rounding	After rounding
$F(x)$	0.1215	0.1217	0.7028	0.7028
$f_1(x)$	1301.5	1281.8	15.2897	15.2694
$f_2(x)$	0.1215	0.1217	0.5554	0.5557
$M_1{}'_{max}$ (N·m)	4.7105	4.7105	4.7105	4.7105
$M_1{}'_{min}$ (N·m)	−7.7005	−7.7005	−7.7005	−7.7005
M_{1max} (N·m)	2.6049	2.5767	4.4244	4.4264
M_{1min} (N·m)	−2.3800	−2.3862	−4.0885	−4.0910
M_{amax} (N·m)	84.7203	84.0963	11.7916	11.7857
M_{amin} (N·m)	−45.7165	−45.3811	−6.2886	−6.2856

data proved that the consideration of reducing the fluctuation of M_a while balancing the fluctuation of M_1 is necessary and worthily.

4.1.2. Example 1.2

Fig.5 shows the results of using the control functions which are gained from example 1.1 to balance the input torque M_1 and M_a of the second crank-rocker mechanism. The data of the results are listed in Tables 3 and 5.

According to the results, the improvements of M_1 in the case $\omega_1 = 0$, $\omega_2 = 1$ are 45.19% and 35.64% for the RMS value and the minimal value respectively, but the maximal value of M_1 is increased from 2.1813(N·m) to 4.1853(N·m). The aim of adding the active balancer is to reduce the fluctuations of M_1. However, in this example, when we use the control function optimized for the first crank-rocker mechanism to balance the second one, the maximal value of M_1 is increased, not reduced. So we should redesign a suitable control function for the second crank-rocker mechanism. In the case $\omega_1 = 0.01$, $\omega_2 = 0.99$, the improvements are 85.19%, 52.80% and

Table 5 The results of the design variables for example 1 and example 2

Example 1.1	$\omega_1=0,\ \omega_2=1$		$X=[1.3731,1878.5,-13367,-3095.2,-43413,-941.95,1.9831\times10^5]$
	$\omega_1=0.01,\ \omega_2=0.99$		$X=[16.818,984.39,-9067.7,-226.4,1.8572\times10^5,41.349,-2.4072\times10^5]$
Example 1.2	$\omega_1=0,\ \omega_2=1$		$X=[1.3731,1878.5,-13367,-3095.2,-43413,-941.95,1.9831\times10^5]$
	$\omega_1=0.01,\ \omega_2=0.99$		$X=[16.818,984.39,-9067.7,-226.4,1.8572\times10^5,41.349,-2.4072\times10^5]$
Example 1.3	$\omega_1=0,\ \omega_2=1$		$X=[12.883,1221.9,-8538.6,88.36,-70726,443.74,-95600]$
	$\omega_1=0.01,\ \omega_2=0.99$		$X=[20.179,594.54,-2619.6,-1275.8,-1.8113\times10^5,1115,-74177]$
Example 2	$\omega_1=0$ $\omega_2=1$	Before rounding	$X=[14.418,1060.1,-9062.7,-226.26,1.8572\times10^5,41.347,-2.4072\times10^5,$ $1\times10^{-6},0.28969,0.14026,1\times10^{-6},1\times10^{-6},1\times10^{-6},41.466,75.466,91.954,17]$
		After rounding	$X=[14.418,1060.1,-9062.7,-226.26,1.8572\times10^5,41.347,-2.4072\times10^5,$ $1\times10^{-6},0.28969,0.14026,1\times10^{-6},1\times10^{-6},1\times10^{-6},41,75,92,17]$
	$\omega_1=0.01$ $\omega_2=0.99$	Before rounding	$X=[14.119,1060.1,-9062.6,-226.24,1.8572\times10^5,41.347,-2.4072\times10^5,$ $1\times10^{-6},0.047416,0.012111,1\times10^{-6},1\times10^{-6},1\times10^{-6},190.83,244.88,250.9,215.6]$
		After rounding	$X=[14.119,1060.1,-9062.6,-226.24,1.8572\times10^5,41.347,-2.4072\times10^5,$ $1\times10^{-6},0.047416,0.012111,1\times10^{-6},1\times10^{-6},1\times10^{-6},191,245,251,216]$

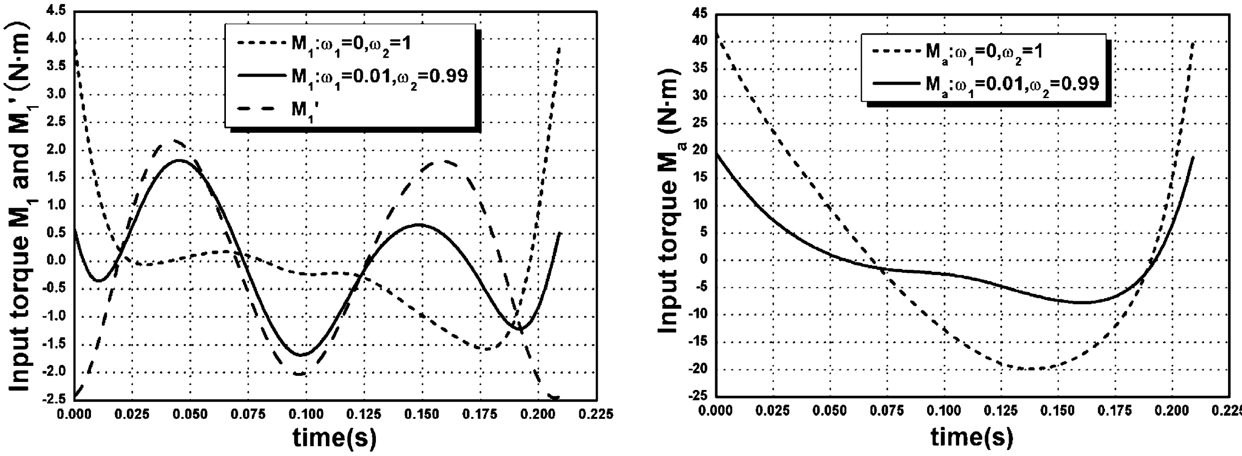

(a) Input torque M_1 and M_1' **(b) Input torque M_a**

Fig. 5. Design results of example 1.2

61.14% for the RMS value, the maximal value and the minimal value of M_a respectively and 57.85%, 16.60% and 31.37% for the RMS value, the maximal value and the minimal value of M_1 respectively.

4.1.3. Example 1.3

In this example, an optimization procedure is taken to redesign the control functions for the second crank-rocker mechanism. The results are shown in Fig.6 and the data are listed in Tables 3 and 5.

According to Fig.6 and Table 3, the improvements of 90.96%, 15.49% and 81.86% are gained for the RMS value, the maximal value and the minimal value of M_1 respectively in the case $\omega_1 = 0$, $\omega_2 = 1$. In the case $\omega_1 = 0.01$, $\omega_2 = 0.99$, the improvements of M_1 are 86.13%, 28% and 64.87% for the RMS value, the maximal value and the minimal value respectively. Similarly, the improvements of 82.98%, 60.28% and 51.73% for the RMS value, the maximal value and the minimal value of M_a respectively are gained by reducing improvements 34.56%, 8.39% and

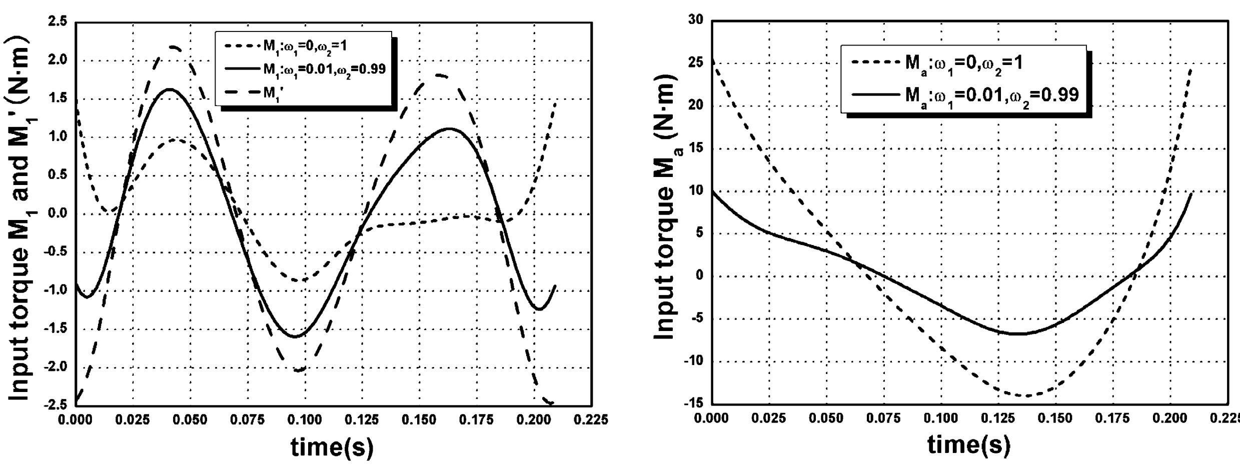

(a) Input torque M_1 and M_1' **(b) Input torque M_a**

Fig. 6. Design results of example 1.3

45.85% for the RMS value, the maximal value and the minimal value of M_1 respectively. Comparing with the results of example 1.2, we can find that the balancing effect of redesigning the control functions for the changed mechanism is better than the effect of using the old control functions.

It is observed from Example 1 that the active balancer can balance the input torque of the changed mechanism all the same by redesigning the control function of the servomotor.

4.2. Example 2

Integrated design of the control function for the servomotor and the structure parameters for the differential gear train is shown in this example. The crank-rocker mechanism and the differential gear train used in this example are the same as example 1.1. Moreover, there are some constraints should be account for. The first one, according to equation (31), we let $\delta = 1 \times 10^{-6}$kg·m^2. The second one, from the analysis of equation (38), we let $k = 1$. The third one, we also eliminate C_8, C_9 and C_{10} in this example. Since the teeth numbers of the gears must be integers, we have to round the data which obtained from the optimization procedure. The curves of the rounded data which are listed in Tables 4 and 5 are displayed in Fig.7.

From the results of the design variables listed in Table 5, it is revealed that J_g, J_d, J_b and J_a are equal to the boundary of the optimization constraints. So we get a conclusion that the optimization results will be better with smaller moments of inertia of the moving parts in the differential gear train except J_{gg} and J_H.With the data listed in Table 4, we can know that the improvements of M_1 are 87.83%, 45.30% and 69.01% of the RMS value, the maximal value and the minimal value respectively in the case $\omega_1 = 0$, $\omega_2 = 1$. The summation of the improvements in this case is 13.83% more than example 1.1. In the case $\omega_1 = 0.01$, $\omega_2 = 0.99$, the improvements of M_1 are 44.43%, 6% and 46.87% for the RMS value, the maximal value and the minimal value respectively. We also get the improvements of 98.81%, 85.99% and 86.15% for the RMS value, the maximal value and the minimal value of M_a respectively by reducing 49.41%, 86.75% and 32.08% for the RMS value, the maximal value and the minimal value of M_1 respectively. The summations of the improvements for M_a and M_1 in this case are 47.95% and 4.18% more than the example 1.1 respectively. These analytical data prove that the integrated design method is better than the approach of just optimizing the control function of the servomotor.

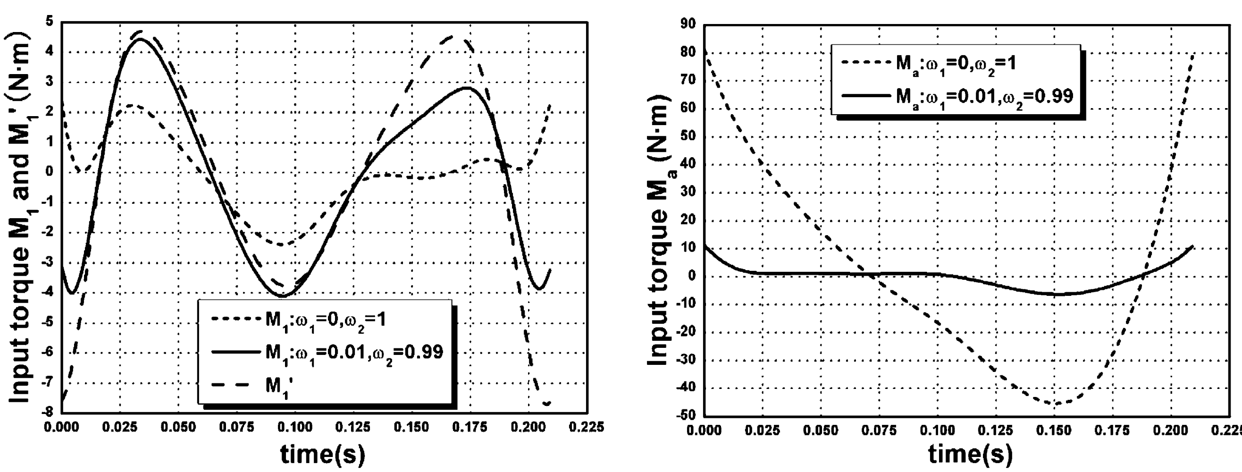

(a) Input torque M_1 and M_1' **(b) Input torque M_a**

Fig. 7. Design results of example 2

As shown in Figs. 4, 5 and 6, the fluctuations of M_a is larger than the fluctuations of M_1. Just like a gear transmission system, the differential gear train is a linear mechanism. The servomotor of the active balancer may need to charge all the nonlinearity of the input torque M_1. This is why the fluctuations of M_a is larger than the fluctuations of M_1. Example 2 shows that parts of the fluctuations of M_a can be reduced through the integrated method.

Moreover, maybe we can use a nonlinear mechanism to help the servomotor for charging parts of the fluctuations of M_1. Through this way, the fluctuations of M_a can be reduced too. As shown in Fig. 8, we can replace the internal gear **b** and the fixed axis gear **d** with a pair of noncircular gears. Parts of the fluctuations of M_1 can be balanced by the noncircular gear pair and the fluctuations of M_a can be reduced accordingly. This configuration also inherits the advantages of the compact structure and the good dynamic performance in the gear transmission system.

5. CONCLUSION

This paper presents a new concept of active balancer which uses a differential gear train and a servomotor to reduce the input torque fluctuations of mechanism. A control function of the servomotor which can eliminate the input torque of the mechanism completely is obtained through the analytical way. An optimization method and an integrated method are proposed to balance the input torque of the working system with minimizing the servomotor's own input torque fluctuation at the same time. It is observed from the results of the examples that satisfactory improvements are gained by using the two approaches.

This active balancer has some characteristics during balancing the input torque. First of all, one of the two input shafts of the differential gear train is coupled with the output shaft of the working mechanism. The structure like this makes the kinematics characteristics of the working mechanism not to be disturbed. Besides, the active balancer is compact in structure and can be installed or uninstalled independently. Furthermore, if the working condition altered, we can balance the input torque all the same by redesigning the control function of the servomotor. In

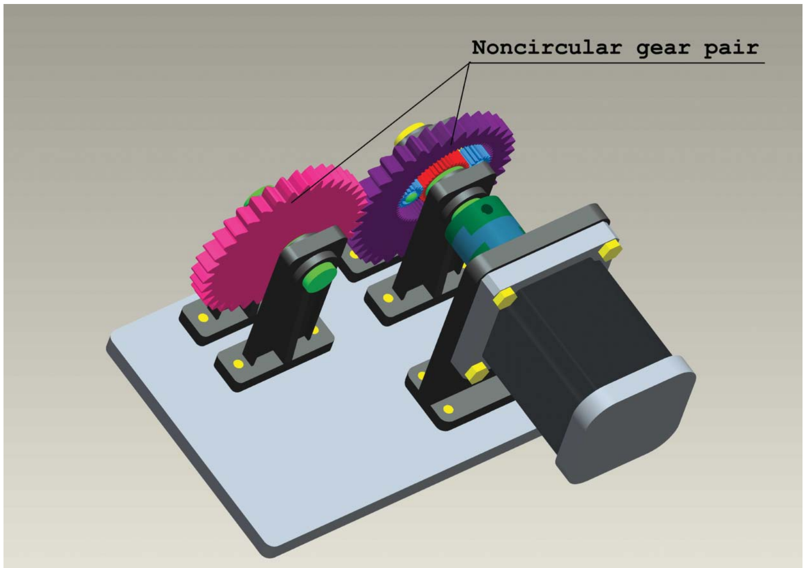

Fig. 8. The active balancer with a pair of noncircular gears

addition, the crank-rocker mechanism used in this paper can be displaced by any other mechanism.

ACKNOWLEDGMENT

This research is sponsored by National Natural Science Foundation of China (No.50405004 and No.50875018).

REFERENCES

1. Berkof, R.S., "The input torque in linkages," *Mech. Mach. Theory*, Vol. 14, No. 1, pp. 61–73, 1979.
2. Kochev, I.S., "General method for active balancing of combined shaking moment and torque fluctuations in planar linkages," *Mech. Mach. Theory*, Vol. 25, No. 6, pp. 679–687, 1990.
3. Liu, D.Y. and Huang, Z., "The input torque balancing of linkage," *Mech. Mach. Theory*, Vol. 24, No. 2, pp. 99–103, 1989.
4. Nishioka, M., "State of the art of torque compensation of dynamic effects," *Proc. of the 6th World Congress on Mech. Mach. Theory*, pp. 713–717, 1996.
5. Nishioka, M., "Direct type torque compensation cam for indexing drive," *Proc. of the 11th World Congress in Mechanism and Machine Science*, pp. 1035–1039, 2004.
6. Funk, W. and Han, J.Y., On the complete balancing of the inertia-caused input torque for plane mechanism, *ASME Design Engineering Technical Conference Computers in Engineering Conference, August, 18–22, Irvine, California, 96-DETC/MECH-1570*, pp. 1–6, 1996.
7. Dooner, D.B., "Use of noncircular gears to reduce torque and speed fluctuations in rotating shafts," *Trans. ASME, Journal of Mechanical Design*, Vol. 119, pp. 299–306, 1997.
8. Yao, Y.A. and Yan, H.S.,"A new method for torque balancing of planar linkages using non-circular gears," *Proc. Instn Mech. Engrs Part C: J Mechanical Engineering Science*, Vol. 217, pp. 495–503, 2003.
9. Demeulenaere, B., Spaepen, P. and De Schutter, J., "Input torque balancing using a cam-based centrifugal pendulum: design procedure and example," *Journal of Sound and Vibration*, Vol. 283, pp. 1–20, 2005.
10. Demeulenaere, B., Spaepen, P. and De Schutter, J., "Input torque balancing using a cam-based centrifugal pendulum: design optimization and robustness," *Journal of Sound and Vibration*, Vol. 283, pp. 21–46, 2005.
11. Demeulenaere, B., *et al.*, "Experimental validation of input torque balancing applied to weaving machinery," *Trans. ASME, Journal of Mechanical Design*, Vol. 130, pp. 022307-(1–10), 2008.
12. Teng, G.L., Fu, H.B. and Zhou, W.Y., "A new method of torque compensation for high speed indexing cam mechanism," *Trans. ASME, Journal of Mechanical Design*, Vol. 121, pp. 319–323, 1999.
13. Wu, C.J. and Angeles, J., "The optimum synthesis of an elastic torque-compensating cam mechanism," *Mech. Mach. Theory*, Vol. 36, pp. 245–259, 1989.
14. Tsay, D.M., Ho, H.C. and Wang, K.C., "Design of torque balancing cams for globoidal cam indexing mechanisms," *Trans. ASME, Journal of Mechanical Design*, Vol. 124, pp. 441–447, 2002.
15. Demeulenaere, B. and De Schutter, J., "Input torque balancing using an inverted cam mechanism," *Trans. ASME, Journal of Mechanical Design*, Vol. 127, pp. 887–900, 2005.
16. Yao, Y.A., Yan, H.S. and Zou, H.J., "Dynamic design of variable speed planar linkages," *Chinese Journal of Mechanical Engineering*, Vol. 18, No. 1, pp. 51–54, 2005.

17. Thuemmel, T., ‘‘Dynamic balancing of linkage by active control with redundant drive,’’ *Proceedings 9th IFTOMM World Congress, Milan, Italy*, Vol. 2, pp. 970–975, 1995.
18. Thuemmel, T. and Brandl, M., Active balancing of joint forces in high-speed linkages by redundant drives and learning control, *Proceedings of the 1996 ASME Design Engineering Technical Conference and Computers in Engineering Conference, Irvine, California*, 1996.
19. Zhang, Y., Yao, Y.A. and Cha, J.Z., ‘‘An independent active balancer for planar mechanisms,’’ *Transactions of Canadian Society for Mechanical Engineering*, Vol. 30, No. 2, pp. 167–190, 2007.